Collision Breeding: A Function of Crystal Moments and Degree of Mixing

An experimental procedure based on continuous crystal seeding was developed which can explicitly determine the fundamental relationship between collision breeding and the leading moments of the crystal size distribution. For the aqueous, cooling crystallization of potassium dichromate, the analysis determined that only the mass moment was successful in correlating observations subject to crystal seeding.

It was also observed that mixing may have a pronounced effect on the nucleation rate but that kinetic orders for collision breeding and growth rate were independent of mixing.

R. M. DESAI
J. W. RACHOW
and
D. C. TIMM

Department of Chemical Engineering
University of Nebraska
Lincoln, Nebraska 68508

SCOPE

Collision breeding is now recognized as the source of nuclei in continuous, mixed suspension, mixed product removal (CSMPR) crystallizers. Since an elucidation of this autocatalytic process is essential for design and control of crystallization systems, this study was initiated to demonstrate an experimental procedure designed to determine an explicit nucleation model in terms of the leading moments of the crystal size distribution.

Although the microscopic mechanism of collision breeding is unknown, Larson et al. (1968) and Rosen and Hulbert (1969) used the total mass of crystals in suspension to correlate nucleation kinetics and crystal size distributions. Powers (1963) proposed the existence of aggregates of solute molecules on crystal surfaces which could form nuclei if displaced from the crystal to the mother liquor. This was experimentally substantiated by Shor and Larson (1971), who suggested that the rate of production of aggregates should be dependent on total crystal surface area. In some cases the site of aggregate formation may be the crystal edge. Thus, there is a basis to expect that either total crystal surface area or edge length would be parameters for correlating nucleation kinetics. However, if crystal collisions furnish the means for displacing aggregates from suspended crystals, nucleation rate should vary with the total number of crystals in suspension.

Current research on CSMPR crystallizers utilize only clear feed. In this case, the moments of the crystal size distribution are proportional to each other. An experimental technique is needed to uncouple the leading moments.

CONCLUSIONS AND SIGNIFICANCE

Product crystals of uniform particle size generally realize a market premium. To control size distributions, an explicit description of their rate of formation and their subsequent rate of enlargement in terms of environmental variables must be known. Dominant variables include the level of dissolved solute concentration, expressed as the degree of supersaturation, and a measurement of the suspended magma phase, generally a leading moment of the crystal distribution.

To determine supersaturation in many inorganic crystallization processes, highly accurate solute concentration measurements of the crystallizer's effluent and of equilibrium must be made, since their magnitudes are similar. In this study consistent, reproducible measurements were obtained through the use of a continuous, differential, recording refractometer, the results of which lead to a correlation of crystal growth rate as a function of supersaturation:

$$G = 4.3 \times 10^3 S^2$$

The level of mixing within the crystallizer did not have an effect on this relationship.

The rate of nucleation was correlated in terms of supersaturation and suspended magma density:

$$B = 9.1 \times 10^6 S M_t^{0.6}$$

It was experimentally verified that suspension density is the correct moment to correlate collision breeding. The other moments of the distribution correlate clear feed observations but fail to correlate seeding observations. Mixing was observed to have an appreciable effect on this kinetic relationship, changing the frequency factor by two to three orders in magnitude, but did not effect the orders of reaction.

The relative dependence on supersaturation of nucleation to growth is significant. If the objective of a crystallization is to produce large sized particles, a plug flow reactor or batch crystallization is preferred to a steady state, continuous mode of operation for those systems in which crystal growth rate is of higher kinetic order than nucleation rate. Since growth and nucleation are parallel, competing reactions, higher levels of supersaturation will result in a proportionately greater deposition of solute on the precipitated, growing phase.

Correspondence concerning this paper should be addressed to D. C. Timm.

Nucleation rate is known to be dependent on the leading moments of the crystal distribution in a continuous, mixed suspension, mixed product removal (CSMPR) crystallizer. However, which of the several moments is dominant remains unknown. Inasmuch as such knowledge is critical for the design and control of crystallization systems, this study was initiated to demonstrate a procedure which is capable of determining an explicit nucleation mechanism in terms of the leading moments of the crystal distribution. The aqueous, cooling crystallization of potassium dichromate was investigated for definitive, illustrative purposes.

SECONDARY NUCLEATION

Crystal nucleation in homogeneous solutions requires a much higher degree of supersaturation than that required for solutions containing a suspended crystalline phase. The heterogeneous, crystalline phase apparently has an autocatalytic effect upon the formation of incipient crystals. Clontz and McCabe (1971) observed that single crystals subjected to fluid shearing forces at intermediate to low levels of supersaturation did not give rise to spontaneous nucleation, but a crystal contact was required to initiate nucleation. When a crystal collided with a surface or with a second crystal, profuse nucleation occurred. Crystal/crystal surface contacts were more fecund than crystal/noncrystal contacts. Crystal edge collisions and sliding contacts proliferated nucleation.

The intrinsic mechanism for collision breeding (Strickland-Constable, 1968) is unknown. Powers (1963) postulated a two-step growth mechanism by which solute aggregates first diffuse to crystal surface regions and then become incorporated into the intricate lattice structure. If the lattice incorporation step is rate determining, a surface zone of partially oriented solute aggregates will develop. Upon collision this partially oriented material is displaced from the crystal mother liquor interface into the bulk of the fluid. If the size of the detached cluster exceeds the critical radius, a nucleus will be formed.

If the rate of collision breeding is relatable to the frequency of collision, secondary nucleation would be expected to correlate with the total number of crystals within the suspended magma. Inasmuch as the critical nucleus size and the extent of aggregate orientation within the boundary layer are functions of supersaturation, supersaturation will also be a variable.

$$B = K_N S^s N_t^p \tag{1}$$

Cayey and Estrin (1967) observed that seed crystals needed to exceed a minimum size before they were nuclei generators. Since the total number of crystals in a steady state CSMPR crystallizer is comprised principally of particles near nuclei in size, an argument exists for the investigation of other nucleation rate models. Shor and Larson (1971) postulated that the surface of the crystal may be composed of a number of active sites, possibly formed by surface imperfections. They reasoned that a surfactant would increase the reactivity of sites, whereas an absorbed ionic impurity would decrease such activity. Experimental observations were consistent with such a model. If it is further reasoned that the number of sites per surface area is constant, the rate of nucleation would be expected to be a function of the total interfacial crystal area as well as the fundamental mass transfer driving force, supersaturation:

$$B = K_A S^w A_t^k \tag{2}$$

Experimental heterogeneous nucleation rates have principally been observed in CSMPR crystallizers at steady state. The assumption that secondary nucleation is dependent upon suspension density has been made (Larson et al., 1968; Rosen and Hulbert, 1969):

$$B = K_M S^y M_t^j \tag{3}$$

Although this model is adequate for correlating published experimental observations, the research to date is not capable of distinguishing between the above nucleation models. In fact, all three mechanisms are equally adequate. The model

$$B = K_L S^u L_t^n \tag{4}$$

will also be considered. Such a model emphasizes the importance of crystal edge length upon collision breeding. If the mechanism is that of microscopic attrition, edges and corners are subjected to a higher degree of abrasion than surfaces.

CRYSTAL DISTRIBUTIONS

Crystal size distributions in a steady state CSMPR crystallizer (Hulbert and Katz, 1964; Randolph and Larson, 1962) are described by

$$G\frac{dn(L)}{dL} + \frac{n(L)}{T} = \frac{n_i(L)}{T} \tag{5}$$

The leading monments of the distribution are defined by the following relationships:

$$\begin{aligned} N_t &= K_n \int_0^\infty n dL \\ L_t &= K_1 \int_0^\infty n L dL \\ A_t &= K_a \int_0^\infty n L^2 dL \\ M_t &= K_m \int_0^\infty n L^3 dL \end{aligned} \tag{6}$$

Clear Feed Observations

For clear feed runs, $n_i(L) = 0$ and Equations (5) and (6) may be integrated, yielding a logarithmic population distribution

$$n(L) = n(0) \exp(-L/GT) \tag{7}$$

and these explicit relationships for the leading moments of the crystal distribution

$$\begin{aligned} N_t &= K_n GT\, n(0) \\ L_t &= K_1 (GT)^2 n(0) \\ A_t &= 2K_a (GT)^3 n(0) \\ M_t &= 6K_m (GT)^4 n(0) \end{aligned} \tag{8}$$

If linear crystal growth rate is assumed to be a power function of supersaturation

$$r = K_g S^a \tag{9}$$

the previous four nucleation models may be expressed in terms of growth kinetics

$$B \propto G^i M^j \tag{10}$$

$$B \propto G^k A^h \tag{11}$$

$$B \propto G^m L^n \tag{12}$$

$$B \propto G^q N^p \tag{13}$$

where

$$B = n(0)G \tag{14}$$

For a CSMPR crystallizer operating at steady state with clear feed, Equations (10) through (13) are not discernible nucleation models. To demonstrate this, Equation (10) will be transformed into Equation (11). Analogous substitutions will transform Equation (10) into Equations (12) and (13).

The last two relationships of Equation (8) may be solved simultaneously to yield

$$M_t \propto (GT)A_t \tag{15}$$

Nucleation rate defined by Equation (10) can therefore be expressed as

$$B \propto G^{i+j} A_t^j T^j \tag{16}$$

To develop a useful working relationship for residence time T, Equations (8) and (15) are solved simultaneously:

$$M_t \propto G^3 T^4 [G\, n(0)] \propto (GT)A_t$$

The substitution of Equation (14) and (10) into this last relation and the subsequent elimination of nucleation rate yields

$$G^2 T^3 G^i (GTA_t)^j \propto A_t$$

Solving for residence time T

$$T \propto A_t^{(1-j)/(3+j)} G^{-(2+i+j)/(3+j)}$$

This relationship may now be substituted for residence time in Equation (16), resulting in

$$B \propto G^{(3i+j)/(3+j)} A_t^{4j/(3+j)}$$

which is Equation (11) where

$$\begin{aligned} k &= (3i + j)/(3 + j) \\ h &= 4j/(3 + j) \end{aligned} \tag{17}$$

Thus Equation (10) is equivalent to Equation (11).

Similarly one can show that

$$\begin{aligned} m &= (2i + 2j)/(2 + 2j) \\ n &= 4j/(2 + 2j) \\ q &= (i + 3j)/(1 + 3j) \\ p &= 4j/(1 + 3j) \end{aligned} \tag{18}$$

Therefore, it is impossible to collect data in a steady state CSMPR crystallizer with clear feed which will elucidate the autocatalytic nucleation mechanism since each model will correlate experimental observations.

Crystal Seeding

In order to determine the dependence of collision breeding on the leading moments of the size distribution, crystal seeding was employed. Stringent control of seed crystal size and quantity introduces additional controllable parameters to the analysis, and the effects of the four leading moments upon collision breeding become discernible.

The size distribution of the crystal population may be calculated from Equation (5) if population density of seed crystals is known. For this work, the distribution of seeds was observed to be exponential with respect to crystal size:

$$\begin{aligned} n_i(L) &= 0 && 0 \leq L < L_1 \\ n_i(L) &= \alpha \exp(-\beta L) && L_1 \leq L \leq L_2 \\ n_i(L) &= 0 && L > L_2 \end{aligned} \tag{19}$$

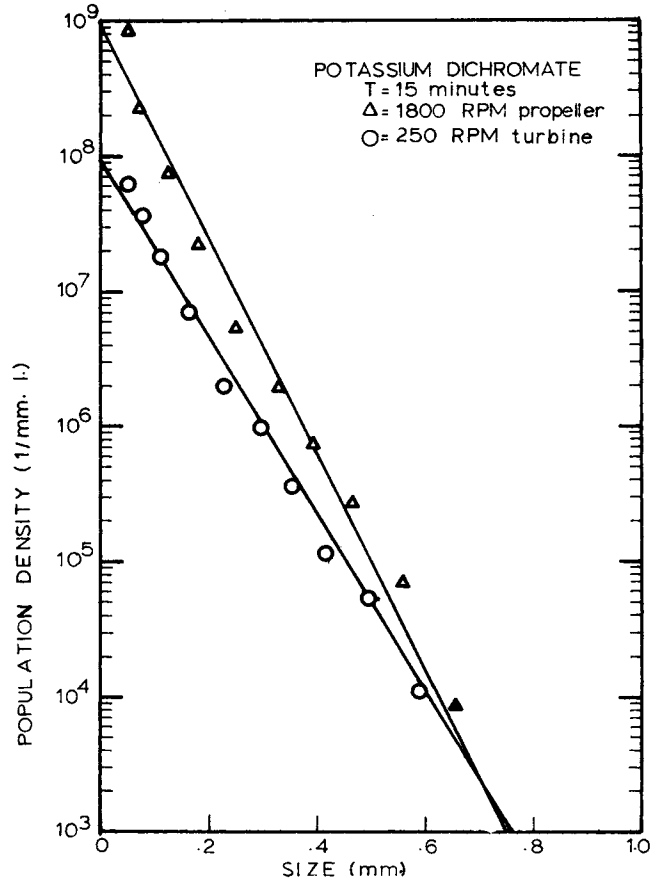

Fig. 1. Effect of mixing on crystal distributions.

The parameter α is relatable to the rate of seeding; the parameter β determines the seed crystals' size dependency; and the limits L_1 and L_2 correspond to their respective minimum and maximum sizes. The theoretical crystal population density for our investigation is, therefore, described by Equation (20):

$$\begin{aligned} n(L) &= n(0) \exp(-L/GT) && 0 \leq L < L_1 \\ \left[n(L) - \frac{n_i(L)}{1 - \beta GT} \right] &= \left[n(L_1) - \frac{n_i(L_1)}{1 - \beta GT} \right] \\ & \qquad \exp[-(L - L_1)/GT] && L_1 \leq L \leq L_2 \\ n(L) &= n(L_2) \exp[-(L - L_2)/GT] \\ & && L > L_2 \end{aligned} \tag{20}$$

Analytical expressions for the leading moments of the distribution may be obtained by integrating Equation (6), using Equation (20) (Desai, 1971). The resultant expressions are sums of exponentials containing the parameters α, β, L_1, and L_2. By judicious experiment design, these four parameters can be manipulated to test the four proposed nucleation models.

MODEL DETERMINATION

The four nucleation models to be tested are expressed in terms of growth kinetics by Equations (10) to (13). Initially i and j will be experimentally determined.

Experiments at Constant Suspension Density

Imposing the experimental constraint of constant suspension density, Equations (10) and (14) can be solved, yielding

$$n(0) \propto G^{i-1} \tag{21}$$

Experimentally the data required are obtained by analysis of steady state observations at different residence times at approximately constant M_t. Steady state size distributions are presented by Figures 1 and 2. In determining the experimental growth rate from the slopes of this graph, a weighted least squares analysis based on the

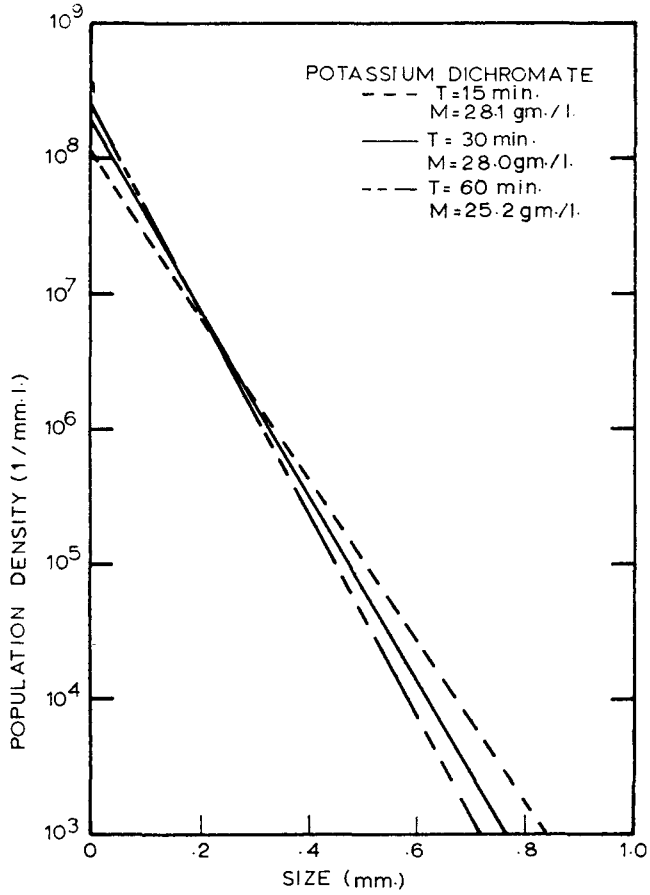

Fig. 2. Effect of residence time on crystal distributions.

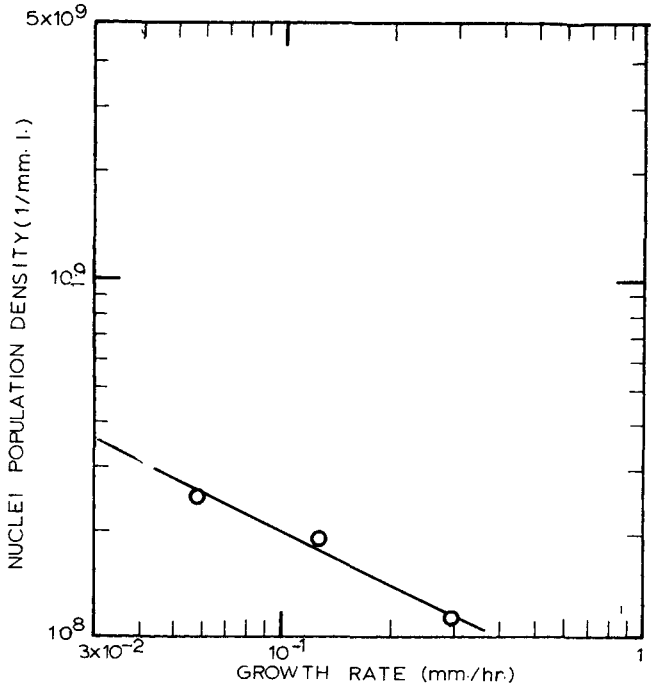

Fig. 3. Nucleation kinetics at approximately constant suspension density.

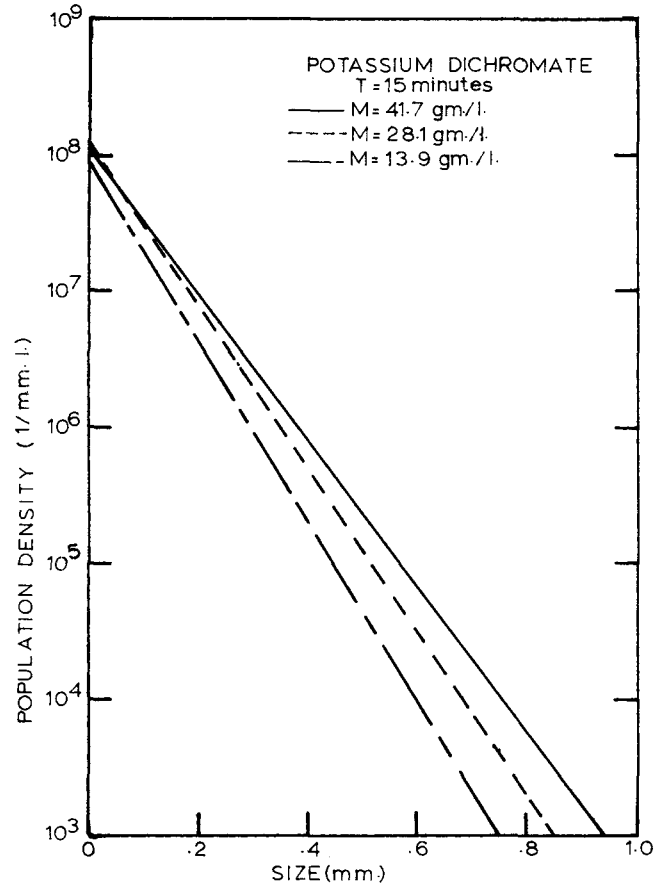

Fig. 4. Effect of solute feed concentration on crystal distributions.

mass of crystalline material contained in a size fraction from a sieve analysis (Rachow, 1969) was used. An initial estimate of i was obtained graphically, utilizing Equation (21), see Figure 3.

Experiments at Constant Residence Time

Having obtained an initial estimate of i, an estimate of j was obtained as follows. Nuclei population density can be eliminated from Equation (14), (10), and the M_t equation of Equation (8). Solving for growth rate yields

$$G \propto M_t^{(1-j)/(i+3)}\, T^{-4/(i+j)} \tag{22}$$

Imposing the experimental constraint of constant residence time, the following relationship applies:

$$G \propto M_t^{(1-j)/(i+3)} \tag{23}$$

Suspension density was varied by changing only the dissolved solute concentration in the feed, and the corresponding size distributions are presented in Figure 4. An estimate for j consistent with Equation (23) was graphically determined from the slope of Figure 5. Having obtained initial estimates for the kinetic orders i and j, the method of successive approximations was used to improve these estimates. This procedure was necessary since small variation in suspension density occurred with changes in residence times. By Equations (10) and (14) nuclei population density can be expressed in terms of growth rate and suspension density:

$$n(0) \propto G^{i-1} M_t^{j} \tag{24}$$

or

$$\ln\left(n(0)/M_t^{j}\right) \propto (i-1) \ln G \tag{25}$$

Utilizing all data from clear feed runs, Equation (25) provides a method for obtaining a new estimate for i.

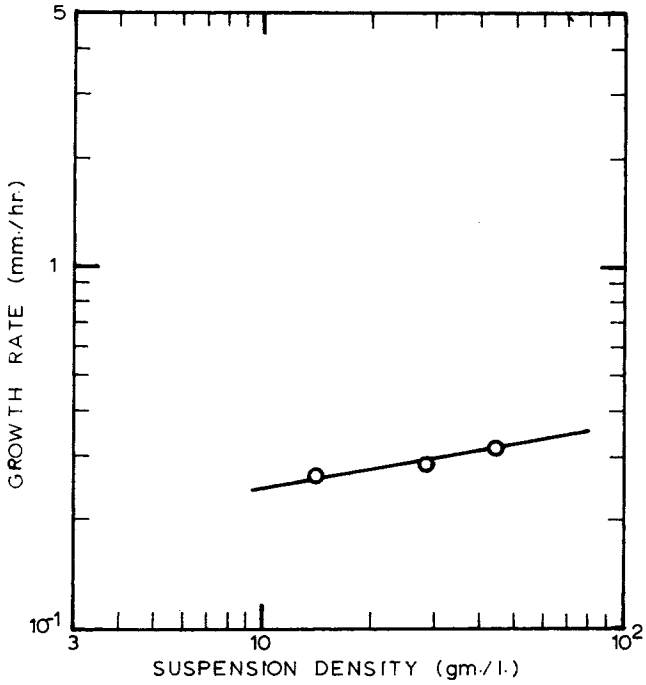

Fig. 5. Nucleation kinetics at constant residence time.

This new estimate for i can be used to improve the estimate for j, utilizing the following relationship:

$$\ln\left(\frac{n(0)}{G^{i-1}}\right) \propto j \ln M_t \qquad (26)$$

This chain of successive approximates can be continued until the two values for the kinetic orders converge. Equations (17) and (18) were then used to estimate the kinetic orders for the other nucleation models.

Nucleation Model Discrimination

To discriminate between the four models, crystal size distribution data were collected for two seeding runs. For one run (see Figure 6) the seeds were in the size range 450 to 586 microns, $\beta = 0.0$ and $\alpha = 5 \times 10^5$ while for the other run (see Figure 7) they varied from 10 to 113 microns, $\beta = 22.5$ and $\alpha = 7 \times 10^9$. In determining the nuclei population density from these figures, growth rate was first determined from supersaturation. Nuclei population density was then determined by a least squares analysis such that the theoretical and actual mass distribution produced a minimum error.

In reference to Equation (26), analogous equations may be derived for the other nucleation models:

$$\ln\left(\frac{n(0)}{G^{i-1}}\right) \propto h \ln A_t$$

$$\ln\left(\frac{n(0)}{G^{m-1}}\right) \propto n \ln L_t \qquad (27)$$

$$\ln\left(\frac{n(0)}{G^{q-1}}\right) \propto p \ln N_t$$

Equations (26) and (27) all fit the experimental clear feed observations, as shown by Figures 8 to 11. It is apparent that the mass moment correlates all observations, clear feed, and seeded runs, whereas the other models do not correlate data from the seeded runs. This decisively shows that mass is the controlling moment and that it exclusively determines the extent of collision breeding.

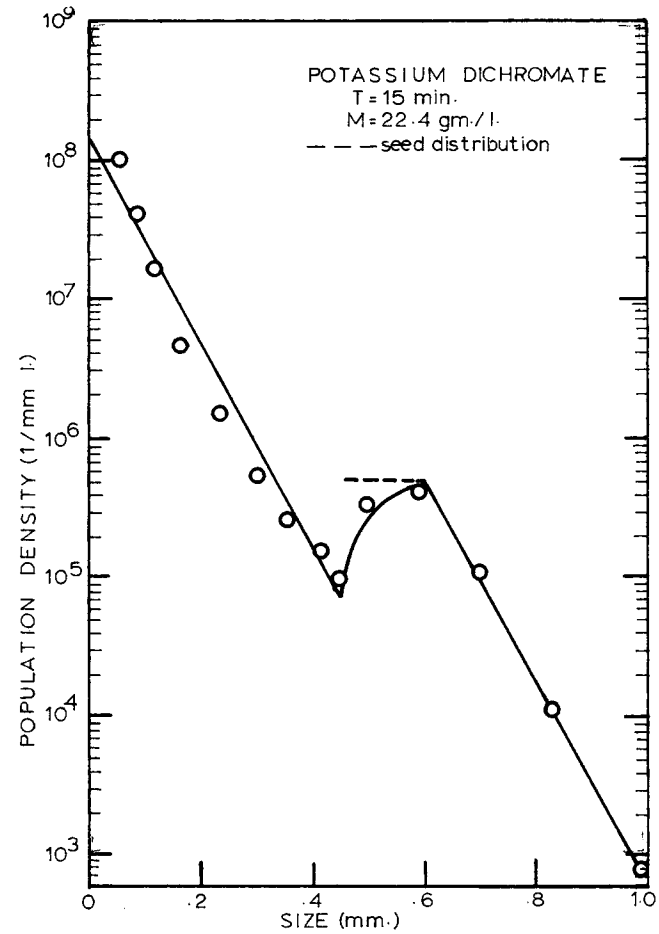

Fig. 6. Effect of seeding on crystal distribution.

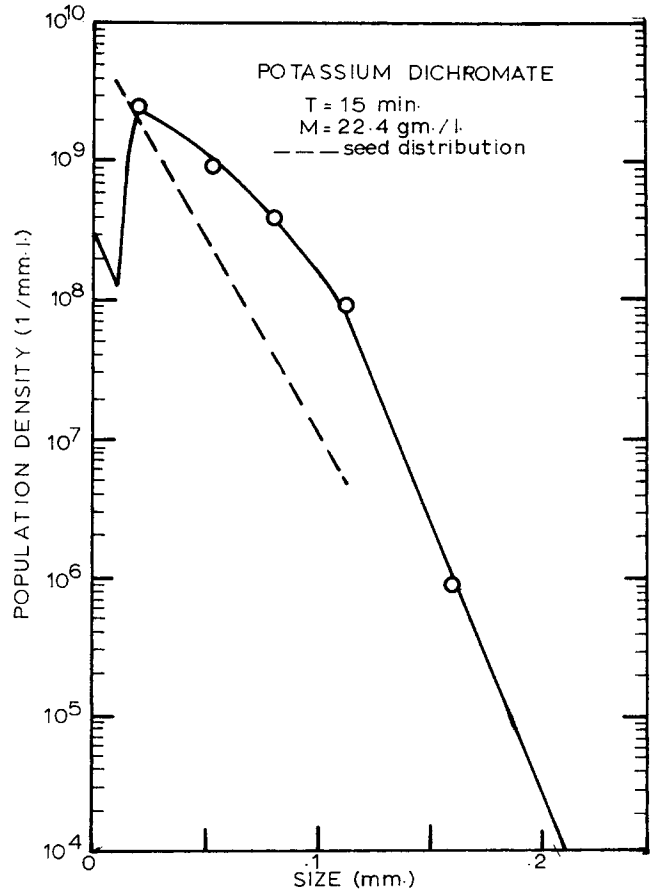

Fig. 7. Effect of seeding on crystal distribution.

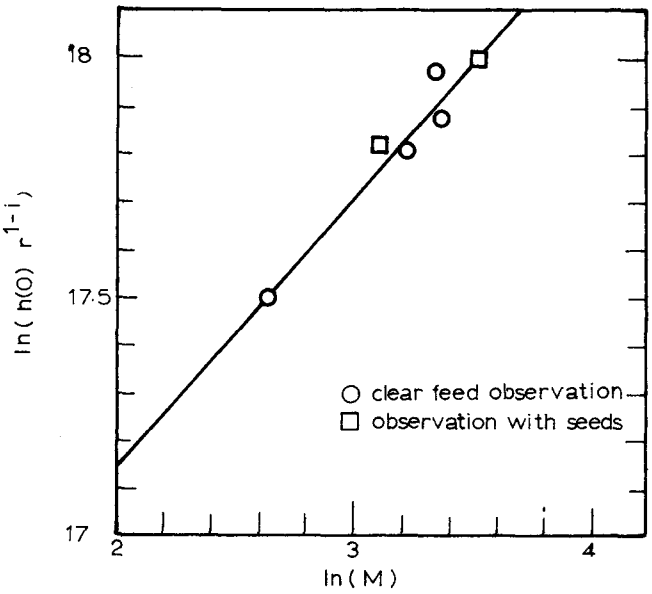

Fig. 8. Test of collision breeding: function of suspension density.

EFFECT OF MIXING ON SIZE DISTRIBUTIONS

The basic cooling crystallization system described by Cooper and Timm (1971) and by Rachow (1969) was used for this investigation. However, major modifications were incorporated into the agitator design. A slow speed turbine (250 rev./min.) with a draft tube and eight baffles (4 inside the draft tube, 4 inside the annulus) was used. The new mixer again resulted in violent mixing, but air entrainment was eliminated. A significant observation with regard to crystal size distribution was made with the new system, see Figure 1. The size distribution obtained with the turbine was significantly different from that of the previous high speed propeller. Inasmuch as Desai (1971) could reproduce observations before the equipment modification, the deviations are real.

In both designs, tracer studies determined that the system was macroscopically well mixed. However, it is apparent from resultant crystal size distributions that crystallization rates were altered.

With the previous high speed agitator, air entrainment was substantial. It is well documented that entrainment may effect nucleation in highly supersaturated solutions. Perhaps an air-liquid interphase is a significant factor in lower supersaturated regions also. It is also conceivable that resultant microscopic changes in fluid/crystal flow patterns and/or crystal/mixer contacting changed the kinetic rates.

Cooper and Timm (1971) previously reported the following rate equations for the cooling crystallization of aqueous solutions of potassium dichromate:

$$B = 3.4 \times 10^{10} S^{0.9}$$

$$G = 3 \times 10^{3} S^{1.7}$$

Supersaturation measurements were made by rough density measurements. Desai (1971) observed the following rate expressions:

$$B = 9.1 \times 10^{6} S M_t^{0.6}$$

$$G = 4.3 \times 10^{3} S^{2}$$

Improved methods for determining supersaturation utilizing a Water's R4 differential refractometer or a Bausch and Lomb dipping refractometer explain the small discrepancy in kinetic orders on supersaturation. The Becker-Doring-Volmer-Frank growth theory as modified by Burton et al. (1951) is consistent with second-order growth kinetics at low levels of supersaturation. At higher levels of supersaturation the model predicts a first order growth rate relationship.

It is worthy to note that for the two sets of experiments growth rates were essentially reproduced and that the relative kinetic order i is numerically equal to one-half for both observations. However, the rate constant

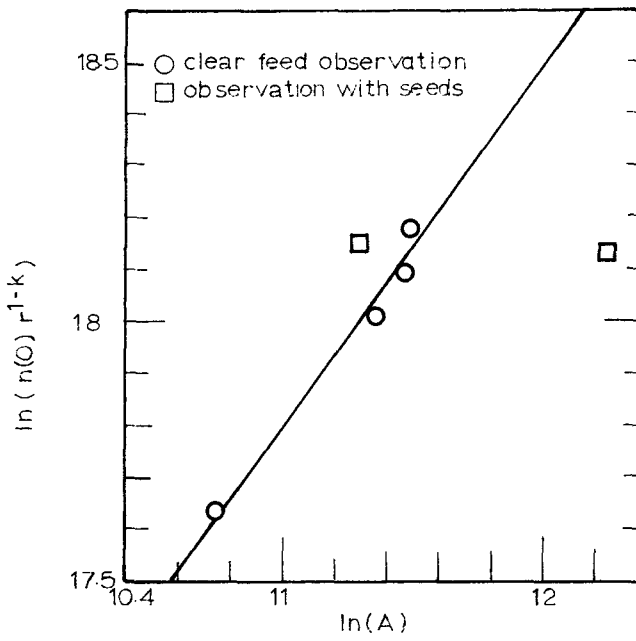

Fig. 9. Test of collision breeding: function of interfacial area.

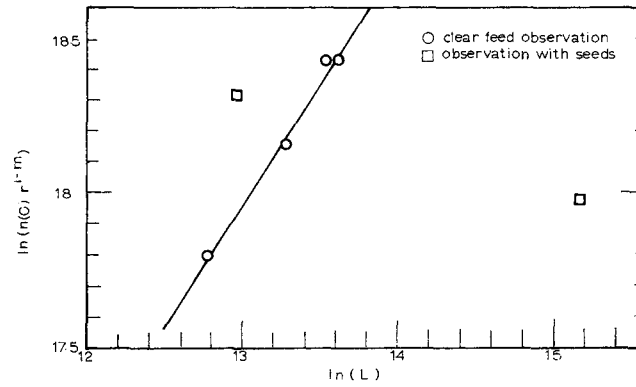

Fig. 10. Test of collision breeding: function of edge length.

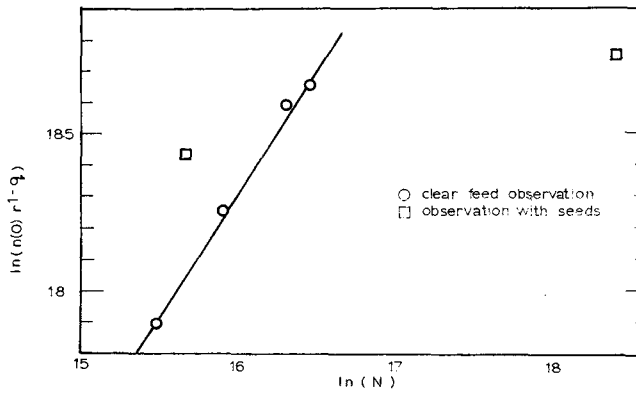

Fig. 11. Test of collision breeding: function of crystal population.

Table 1. Summary of Experimental Observations

Run no.	1	2	4	5	6	7	8
$T_{(min.)}$	60	30	15	15	15	15	15
$n(0) \times 10^{-8}$ no./mm-liter	2.425	1.898	1.117	0.8053	1.037	1.400	2.85
G mm/hr.	0.0582	0.1271	0.2904	0.2640	0.3260	0.2400	0.044
M_t g/liter	25.20	27.98	28.08	13.87	41.70	33.20	22.40
$A_{t_2} \times 10^{-5}$ cm²/liter	0.9560	0.9740	0.8540	0.4630	1.123	0.8142	2.089
$L_t \times 10^{-6}$ cm/liter	0.8210	0.7660	0.5880	0.3510	0.6890	0.4282	3.945
$N_t \times 10^{-7}$ no./l	1.410	1.206	0.8110	0.5310	0.8450	0.6124	9.746
$S \times 10^2$ g/g	0.5250	—	1.170	1.113	—	1.100	0.6050

for nucleation kinetics was observed to change by several orders of magnitude. Thus it is apparent that mixing had a pronounced effect on the rate of collision breeding.

DISCUSSION

To determine the extent of initial breeding, a weighed quantity of crystal seeds were violently suspended in an ammonium thiocyanate/isopropanol electrolyte and then analyzed for small particles with a thousand channel particle analyzer (Kothari, 1971). A peak was observed at about 5 microns and corresponded to a crystallizer population density of the order of 10^4. The experimental population density of these particles in the crystallizer was of the order of 10^8. Therefore, initial breeding was deemed insignificant and was deleted from the analysis. Microscopic observations of the crystals failed to identify dendritic growth centers. Inasmuch as the crystals were well-formed, polycrystalline breeding was assumed negligible.

Observing Table 1, it may be seen how seeding has disturbed the normal trend of the variation in the crystal moments. In Run 7, for example, the mass moment is greater than that of Run 1 while the other moments are significantly less. Specifically, the number moment is approximately half that of Run 2. In Run 8 the mass moment is relatively low while the other moments are considerably greater compared to other runs, the number moment being almost a factor of 10 greater. Such significant relative variation in the moments through seeding made it practical to determine the controlling moment. The number, edge-length, and area moments are not suitable correlating parameters for collision breeding for this system.

The significance of the mass moment in collision breeding may be more difficult to comprehend than physical arguments favoring the other moments. However, if an energy barrier exists for a cluster to be detached from the crystal interface, the rate of embryo formation can be expected to be dependent upon the energy supplied. In the present study, crystal/crystal and crystal/surface collisions are frequent. A readily available form of energy is the kinetic energy associated with collisions. In vigorously agitated suspensions where hindered settling exists, velocities of crystals are expected to be nearly independent of size. Thus kinetic energy of the crystals will be proportional to their mass. However, only a portion of the clusters formed will exceed the critical nucleus size, the remaining embryos will dissociate. In addition, solute concentration, surfactants and ionic impurities are expected to have a pronounced effect on the microscopic development of the crystal-liquid interface. Thus, nucleation is expected to be a function of mass, supersaturation and impurity concentrations.

NOTATION

A_t = total surface area of crystalline phase, mm²/liter
a = kinetic order for growth rate
B = nucleation rate due to collision breeding, no./hr. liter
G = linear crystal growth rate, dL/dt, mm/hr.
i = relative kinetic order for nucleation rate, $i = y/a$
J = nucleation rate due to collision breeding, no./hr. liter
j = kinetic order of collision breeding with respect to suspension density
K_A = nucleation rate constant, crystal area dominant
K_a = crystal area shape factor
K_g = linear crystal growth rate constant
K_L = nucleation rate constant, crystal edge length dominant
K_1 = crystal edge length shape factor
K_N = nucleation rate constant, crystal number dominant
K_n = crystal number shape factor
K_M = nucleation rate constant, crystal mass dominant
K_m = crystal mass shape factor
k = relative kinetic order for nucleation rate, $k = w/a$
L = characteristic dimension of a crystal, mm
L_t = total edge length of crystalline phase, mm/liter
h = kinetic order of collision breeding with respect to crystalline area
M_t = mass concentration of crystalline phase, g/liter
m = relative kinetic order for nucleation rate, $m = u/a$
N_t = number concentration of suspended crystals, no./liter
n = kinetic order of collision breeding with respect to edge length
$n(L)$ = crystal population density, no./mm liter
$n_i(L)$ = seed crystal population density, no./mm liter
q = relative kinetic order for nucleation rate, $q = s/a$
p = kinetic order of collision breeding with respect to crystal number
S = supersaturation, g solute/g solvent
s = kinetic order of collision breeding, crystal numbers dominant
T = residence time
u = kinetic order of collision breeding, crystal edge length dominant
w = kinetic order of collision breeding, crystal area dominant
y = kinetic order of collision breeding, crystal mass dominant

Greek Letters

α = parameter related to seeding rate, no./mm liter
β = parameter describing seed size distribution, mm^{-1}

LITERATURE CITED

Burton, W. K., N. Cabrera, and F. C. Frank, "Growth of Crystals and Equilibrium Structure of Their Surfaces," *Phil. Trans. Roy. Soc. London*, **A 243**, 229 (1951).

Cayey, N. W., and J. Estrin, "Secondary Nucleation in Agitated, Magnesium Sulfate Solutions," *Ind. Eng. Chem. Fundamentals*, **6**, 13 (1967).

Clontz, N. A., and L. W. McCabe, "Contact Nucleation of Magnesium Sulfate Heptahydrate," *Chem. Eng. Progr. Symp. Ser.*, **67**, 6 (1971).

Cooper, T. R., and D. C. Timm, "Crystallization: Kinetics and Design Consideration," *AIChE J.*, **17**, 285 (1971).

Desai, R. M., "The Effect of Crystal Moments on Secondary Nucleation," unpublished M.S. Thesis, Univ. Nebraska-Lincoln (1971).

Hulburt, H. M., and S. Katz, "Continuous Crystallization," *Chem. Eng. Sci.*, **191**, 555 (1964).

Kothari, I. R., "Growth of Single Cells of *Schizosaccharomyces pombe* under Nutrient Limitation," unpublished M. S. Thesis, Univ. Nebraska-Lincoln (1971).

Larson, M. A., D. C. Timm, and P. R. Wolff, "Effect of Suspension Density on Crystal Size Distribution," *AIChE J.*, **14**, 448 (1968).

Powers, H. E. C., "Nucleation and Early Crystal Growth," *Ind. Chem.*, **39**, 351 (1963).

Rachow, J. W., "Steady State Nucleation Kinetics of Aqueous Potasium Dichromate," unpublished M.S. thesis, Univ. Nebraska-Lincoln (1969).

Randolph, A. D., and M. S. Larson, "Transient and Steady State Size Distributions in Continuous Mixed Suspension Crystallizers," *AIChE J.*, **8**, 639 (1962).

Rosen, H. N., and H. M. Hulburt, "Growth Rate of Potassium Sulfate in a Fludized-Bed Crystallizer," *Chem. Eng. Progr. Symp. Ser.*, **67**, 27 (1971).

Shor, S. M., and M. A. Larson, "Effect of Additives of Crystallization Kinetics," *Chem. Eng. Progr. Symp. Ser.*, **67**, 32 (1971).

Strickland-Constable, R. F., *Crystallization*, p. 112, Academic Press, New York (1968).

Ting, H. H., and W. L. McCabe, "Supersaturation and Crystal Formation in Seeded Solution," *Ind. Eng. Chem.*, **26**, 1201 (1934).

Manuscript received May 22, 1973; revision received September 4 and accepted September 5, 1973.

A Theoretical Model for Enzymatic Catalysis Using Asymmetric Hollow Fiber Membranes

The behavior of an immobilized enzyme reactor utilizing asymmetric hollow fibers is simulated using a theoretical model. In this reactor, an enzyme solution contained within the annular open-cell porous support structure of the fiber is separated from a substrate flowing through the fiber lumen by an ultrathin dense membrane impermeable to enzyme but permeable to substrate and product. The coupled set of model equations describing the behavior of this reactor represents an extended Graetz problem in the fiber lumen, with diffusion through the ultrathin fiber skin and reaction in the microporous sponge region. Exact analytic expressions for substrate concentration profiles throughout an idealized fiber which incorporate the membrane and hydrodynamic mass transfer resistances are obtained for a first-order enzyme reaction, and numerical techniques for their evaluation are given. This analysis is extended to yield a numerical finite difference solution for nonlinear Michaelis-Menten reaction kinetics, which is shown to agree with the analytic solution, as K_m/C_0, the ratio of the Michaelis constant to the initial substrate concentration, becomes large (> 100).

LARRY R. WATERLAND
ALAN S. MICHAELS
and
CHANNING R. ROBERTSON

Department of Chemical Engineering
Stanford University
Stanford, California 94305
and the
Alza Research Corporation
Palo Alto, California 94304

SCOPE

In recent years the potential applications of enzymatic catalysis in numerous diverse areas of chemical technology have become apparent. This in turn has brought about a need to develop and characterize new techniques for enzyme immobilization concomitant with the design of efficient immobilized enzyme reactors. Immobilized en-

Correspondence concerning this paper should be addressed to C. R. Robertson.